ADVANCED FUNCTIONAL MATERIALS

FULL PAPER

DOI: 10.1002/adfm.200600921

Ambipolar Conductive 2,7-Carbazole Derivatives for Electroluminescent Devices**

By *Jiun-Yi Shen*, *Xiang-Lin Yang*, *Tai-Hsiang Huang*, *Jiann T. Lin*,* *Tung-Huei Ke*, *Li-Yin Chen*, *Chung-Chih Wu*,* and *Ming-Chang P. Yeh**

A series of 2,7-disubstituted carbazole (2,7-carb) derivatives incorporating arylamines at the 2 and 7 positions are synthesized via palladium-catalyzed C–N or C–C bond formation. These compounds possess glass transition temperatures ranging from 87 to 217 °C and exhibit good thermal stabilities, with thermal decomposition temperatures ranging from 388 to 480 °C. They are fluorescent and emit in the purple-blue to orange region. Two types of organic light emitting diodes (OLEDs) were constructed from these compounds: (I) indium tin oxide (ITO)/2,7-carb (40 nm)/1,3,5-tris(*N*-phenylbenzimidazol-2-yl)benzene (TPBI, 40 nm)/Mg:Ag; and (II) ITO/2,7-carb (40 nm)/tris(8-hydroxyquinoline) aluminum (Alq_3, 40 nm)/Mg:Ag. In type I devices, the 2,7-disubstituted carbazoles function as both hole-transporting and emitting material. In type II devices, light is emitted from either the 2,7-disubstituted carbazole layer or Alq_3. The devices appear to have a better performance compared to devices fabricated with their 3,6-disubstituted carbazole congeners. Some of the new compounds exhibit ambipolar conductive behavior, with hole and electron mobilities up to 10^{-4} $cm^2 V^{-1} s^{-1}$.

1. Introduction

Small organic molecules[1] and organic conjugated polymers[2] used in organic and polymer light emitting diodes (OLEDs and PLEDs) are considered promising candidates for flat-panel displays since the reports from the Kodak team[3] and the Cambridge group.[4] The application of organic electroluminescence (OEL) in flat-panel displays and portable electronic devices has become realistic because of considerable progress in the past decade. To compete with liquid-crystal displays (LCDs), OEL devices have to be low-cost and have to exhibit high performance, high efficiency, and durability. Efficient blue, green, and red emitters with excellent color purity are important for full-color displays. On the other hand, the amorphous character of the materials is also important because it reduces crystallization during long-term operation of the devices.[5] Shirota demonstrated that organic π-electron star-shaped molecules have a strong tendency to form amorphous glasses.[1a] A systematic investigation of a series of symmetric and asymmetric triarylamines by Thompson and co-workers indicated that the incorporation of arylamines in the conjugated segments is beneficial to glass formation.[6] We have been interested in developing amorphous materials that possess high glass-transition temperatures (T_gs) and a high thermal stability for OLED applications. In a series of reports, we found that encapsulation of a carbazolyl moiety with diarylamines at the 3 and 6 positions led compounds with high T_gs and thermal decomposition temperatures (T_ds).[7] Furthermore, these compounds are emissive with color tunability.

Recently, 2,7-substituted carbazole compounds were reported to have a higher level of conjugation than their 3,6-disubstituted counterparts.[8] It is therefore interesting to examine how the 2,7-substituted carbazoles (Scheme 1, **A**) differ in physical properties from their 3,6-disubstituted analogues (Scheme 1, **B**) and if they retain good morphological and thermal characteristics, i.e., high T_gs and T_ds. There is a substantial number of studies on 3,6-disubstituted carbazole compounds, including

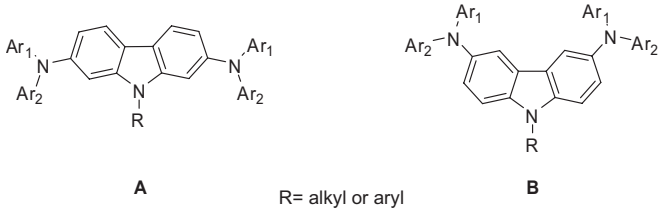

Scheme 1. Two isomers of carbazole derivatives.

[*] Dr. J. T. Lin, J.-Y. Shen, T.-H. Huang
Institute of Chemistry, Academia Sinica
Taipei 115, Taiwan (ROC)
E-mail: jtlin@chem.sinica.edu.tw
Dr. J. T. Lin
Department of Chemistry, National Central University
Chungli 320, Taiwan (ROC)
Dr. C.-C. Wu, T.-H. Ke, L.-Y. Chen
Graduate Institute of Electro-optical Engineering and
Graduate Institute of Electronics Engineering
Department of Electrical Engineering, National Taiwan University
Taipei 106, Taiwan (ROC)
E-mail: chungwu@cc.ee.ntu.edu.tw
Dr. M.-C. P. Yeh, X.-L.Yang
Department of Chemistry, National Taiwan Normal University
Taipei 117, Taiwan (ROC)
E-mail: cheyeh@scc.ntnu.edu.tw

[**] We thank the Academia Sinica, National Taiwan University, National Taiwan Normal University, and the National Science Council for supporting this work.

small molecules, oligomers, and polymers[9] for OLED applications. However, there are only a few studies on low-molecular-weight 2,7-disubstituted carbazole compounds thus far. The main obstacle is the lack of an efficient synthesis procedure for these compounds. Recently Leclerc and co-workers[10] and Müllen and co-workers[11] reported new synthetic pathways towards 2,7-dihalocarbazoles, which are convenient precursors for carbazole-based optoelectronic materials. Herein, we report the synthesis and characterization of small-molecule 2,7-disubstitued carbazole materials with peripheral diarylamines. Devices fabricated from these materials will also be discussed.

2. Results and Discussion

2.1. Synthesis of the Materials

The structures of the new 2,7-disubstituted carbazole (2,7-carb) derivatives and some of their 3,6-disubstituted (3,6-carb) analogues (e.g., **7A** and **9A**) are illustrated in Figure 1. Two dif-

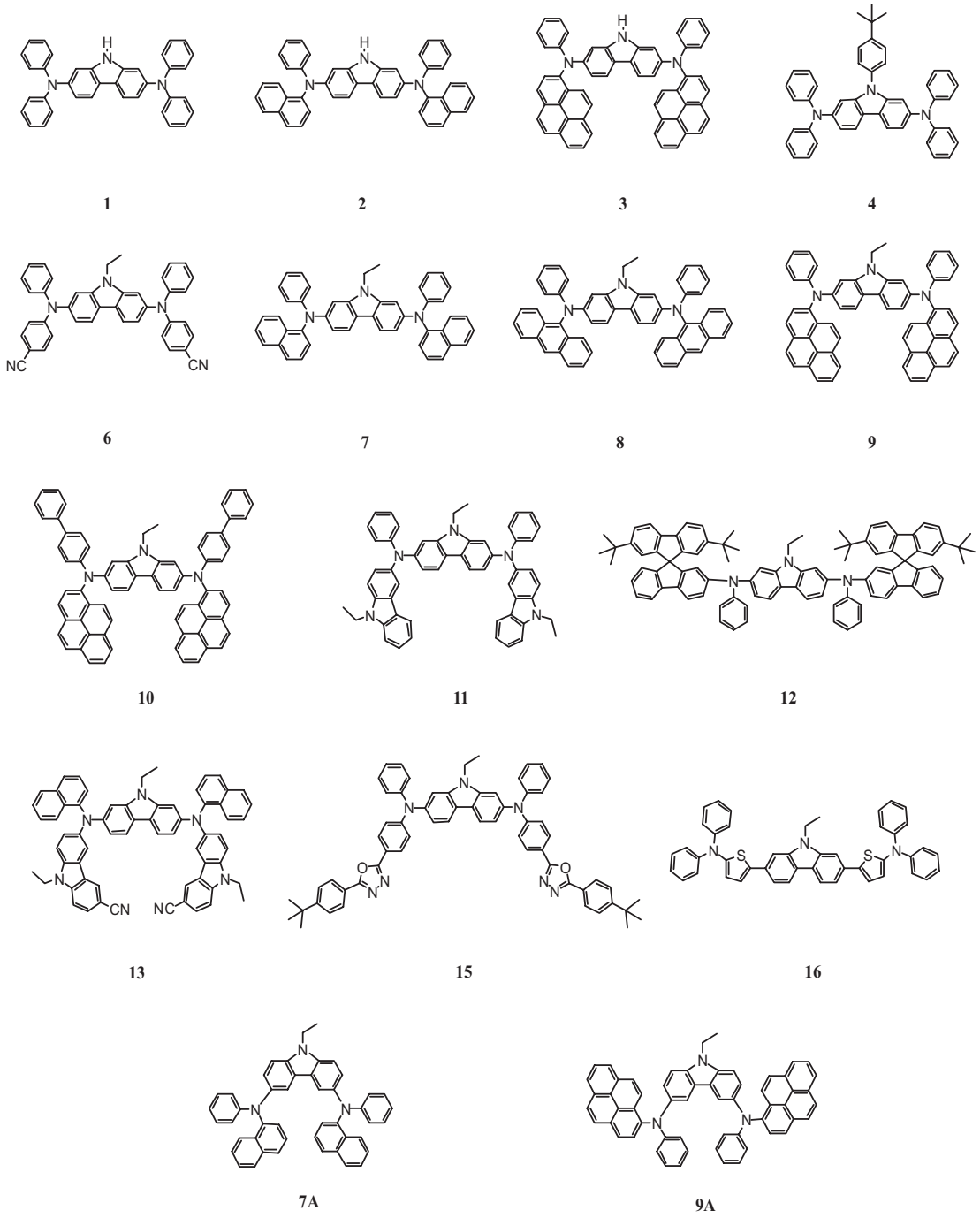

Figure 1. Structures of the compounds used in this study.

ferent pathways for the synthesis of the compounds are outlined in Scheme 2. Compounds **1**–**4** were synthesized via the first route, which consisted of a palladium-catalyzed aromatic C–N coupling reaction[12] of 4,4′-dibromo-2-nitrobiphenyl[11] with secondary arylamines to provide the intermediate **I**, followed by an in situ reductive Cadogan ring-closure of **I** in the presence of triethyl phosphite to obtain **1**–**3**. Subsequently, compound **1** underwent a facile Ullmann C–N coupling reaction[13] with 1-bromo-4-*tert*-butylbenzene in the presence of Cu/K_2CO_3 in nitrobenzene to give compound **4**. Compounds **6**–**13** were synthesized via the second route, comprising N-alkylation of 2,7-dibromo-9*H*-carbazole[11] with 2-bromoethane to form **5**, followed by a palladium-catalyzed aromatic C–N coupling reaction of **5** with diarylamines. A Stille cross-coupling

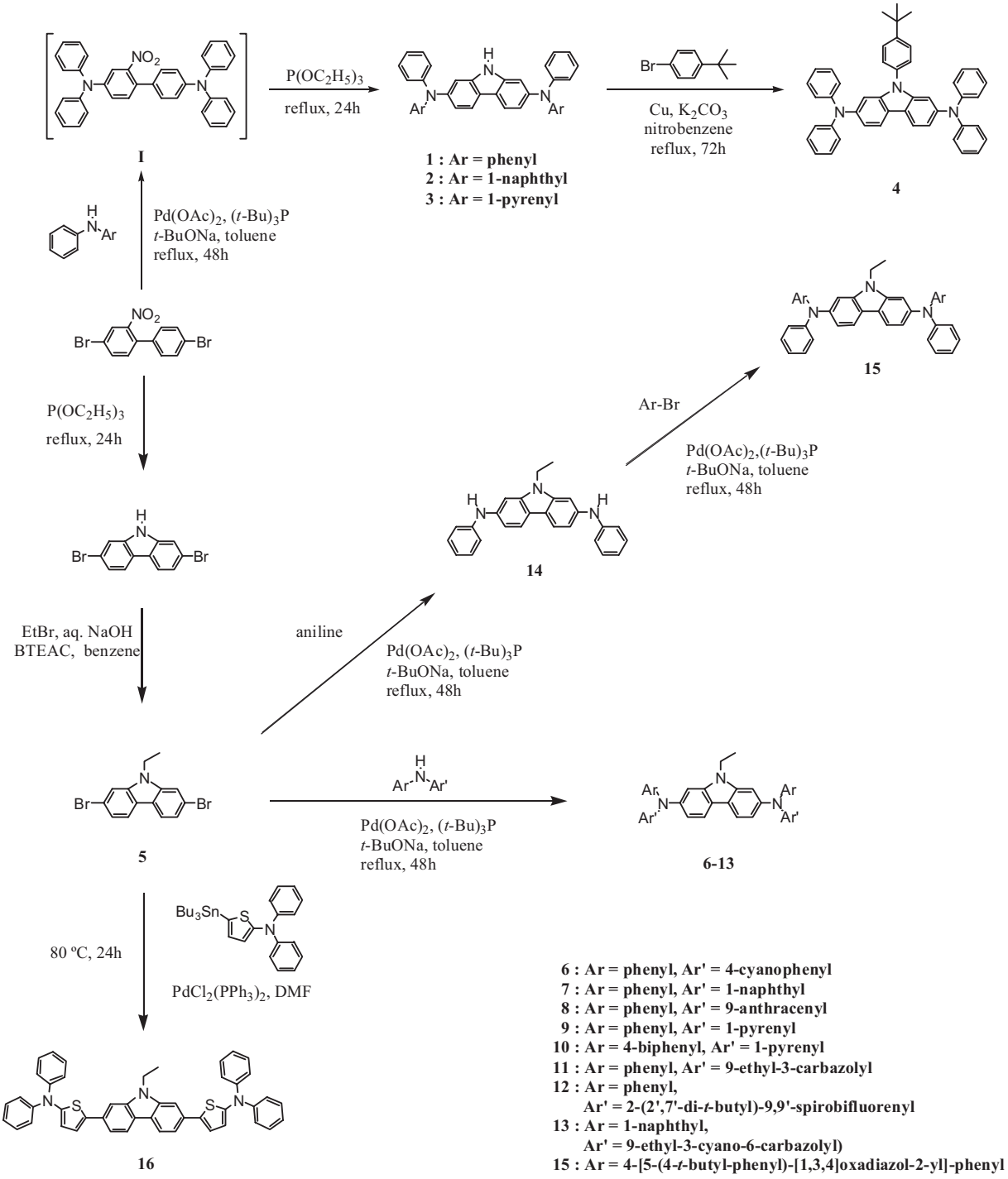

Scheme 2. Outline of the synthetic scheme. Ac: acyl, Ar: aryl, *t*-Bu: *tert*-butyl, Et: ethyl, BTEAC: benzyltriethylammonium chloride, Ph: phenyl, DMF: *N,N*-dimethylformamide.

reaction of compound **5** with 5-[*N*,*N*-diphenylamino]-2-(tri-*n*-butylstannyl)thiophene yielded compound **16**.

2.2. Thermal Properties

The glass-forming capabilities and thermal stabilities of the materials were determined by differential scanning calorimetry (DSC) and thermogravimetric analysis (TGA). The detailed data are collected in Table 1. The T_d values of these compounds, under N_2 atmosphere, range from 388 to 490 °C. Compounds **1**, **6**, **8**, and **16** exhibited melting isotherms (T_m: **1**, 228 °C; **6**, 283 °C; **8**, 302 °C; **16**, 178 °C) during the first heating cycle, but rapid cooling of the melt led to the formation of a glassy state that persisted in subsequent heating cycles. All other compounds exhibited a glass transition in the first heating cycle, and no crystallization exotherm and melting endotherm were noticed. With the same peripheral diarylamine substituents, replacement of the *N*-H substituent by an *N*-aryl or *N*-ethyl group leads to a decrease of T_g (**1**→**4**, **2**→**7**, and **3**→**9**). Aside from the higher rotational freedom of the ethyl and *t*-butyl group, we presume that N–H···N–H or N–H···π hydrogen bonds in the N–H compounds also plays an important role.

For the 2,7-disubstituted carbazole derivatives in this study, the role of carbazole in raising the T_g is evident when comparing **1** (T_g = 109 °C) or **4** (T_g = 100 °C) with a commonly used hole-transport material such as 1,4-bis(diphenylamino)biphenyl (DDB, T_g = 77 °C), and when comparing **2** (T_g = 133 °C) or **7** (T_g = 111 °C) with 1,4-bis(1-naphthylphenylamino)-biphenyl (NPB, T_g = 95 °C).[14] Furthermore, the incorporation of a 2-spirobifluorenyl,[15] 1-pyrenyl,[7a] or 6-cyano-3-carbazolyl[15] moiety dramatically raises the T_g value of the compound, consistent with our previous observations. Comparison of T_g values between compounds **6** (123 °C), **7** (111 °C), **8** (166 °C), **9** (171 °C), **11** (155 °C), **12** (210 °C), and **15** (169 °C) shows that the order of effectiveness in raising T_g is 2-spirobifluorenyl > 1-pyrenyl > 4-[5-(4-*tert*-butyl-phenyl)-[1,3,4]oxadiazol-2-yl]-phenyl > 9-anthracenyl > 3-carbazolyl > 4-cyanophenyl > 1-naphthyl. The increasingly restricted motion,[16] higher molecular mass,[17] and increasing polar nature[18] of the compounds all contribute to the observed increase of the T_g values. The 2,7-disubstituted carbazole compounds appear to have slightly lower T_g values than their 3,6-disubstituted counterparts, i.e., **7** (111 °C) < **7A** (120 °C) and **9** (171 °C) < **9A** (174 °C). The T_d values of the 2,7-disubstituted carbazole compounds (**7**, 388 °C; **9**, 490 °C) do not differ strongly from those of the 3,6-disubstituted compounds (**7A**, 385 °C;[19] **9A**, 510 °C).

Table 1. Physical data for compounds **1**–**16**, **7A**, and **9A**.

Compound	T_g [a] [°C]	T_d [b] [°C]	λ_{max} [c] [nm]	λ_{em} (ϕ_f) [d] [nm]	E_{ox} (ΔE_p) [e] [mV]	HOMO/LUMO [f] [eV]
1	109	390	375, 312, 262	400 (0.74), 401	80 (94), 391 (96)	4.88/1.75
2	133	403	368, 260	500 (0.17), 456	100(99), 434 (94)	4.90/1.89
3	191	487	417, 366, 360, 338, 323, 276	550 (0.07), 500 (0.38)	114 (85), 425 (94), 1034 (i)	4.91/2.24
4	100	388	375, 361, 308, 273	401 (0.85), 403	162 (108), 457 (105)	4.96/1.85
6	123	448	372, 366, 329, 278	493 (0.09), 430	385 (109), 577 (109)	5.19/2.14
7	111	388	373, 271	498 (0.24), 460 (0.25)	125 (94), 471 (93)	4.92/1.91
8	166	418	444, 375, 360, 250	596 (0.01), 560	146 (85), 509 (97), 1038 (i)	4.94/2.44
9	171	490	419, 366, 337, 323, 276, 266	551 (0.32), 495 (0.32)	119 (130), 461 (137), 1042 (i)	4.92/2.24
10	196	454	424, 380, 336, 324, 275, 266	542 (0.18), 503 (0.35)	119 (90), 430 (89), 1032 (i)	4.92/2.33
11	155	465	378, 314, 283	430 (0.19), 431	-21 (112), 228 (85), 782 (51), 871 (i)	4.78/1.83
12	210	460	392, 363, 353, 315, 302, 276	416 (0.74), 419	98 (85), 424 (84)	4.90/1.91
13	217	480	368, 298	513 (0.15), 467	25 (89), 348 (89)	4.83/1.87
15	169	440	386, 359, 276	522 (0.17), 452	279 (95), 517 (100)	5.08/2.17
16	87	430	405, 297, 266	481 (0.35), 462	177 (131)	4.96/2.26
7A	120	385	351, 278, 257	497 (0.05), 456 (0.13)	127 (78), 518 (76), 1164 (i)	4.93/2.00
9A	174	510	408, 328, 274	548 (0.03), 509 (0.35)	116 (63), 448 (74), 1012 (i)	4.91/2.33

[a] Obtained by DSC under N_2. [b] Obtained by TGA under N_2. [c] In CH_2Cl_2 solution. [d] In CH_2Cl_2 (first value) and toluene, ϕ_f: fluorescence quantum yield, relative to coumarin 1 (99 % in ethyl acetate) or coumarin 6 (63 % in acetonitrile). Corrected for solvent refractive index changes. [e] In CH_2Cl_2. All E_{ox} data are relative to ferrocene (E_{ox} 260 mV relative to Ag/Ag^+). Concentrations: 10^{-3} M; scan rate: 100 mV s^{-1}; i: irreversible. [f] Highest occupied molecular orbital (HOMO) energy calculated with reference to ferrocene (4.8 eV). A solvent-to-vacuum correction was not applied. The bandgap was determined from the observed optical edge, and the lowest unoccupied molecular orbital (LUMO) energy was derived from the relation bandgap = HOMO–LUMO.

2.3. Electrochemical Properties

Electrochemical characteristics of the 2,7-disubstituted carbazole derivatives were studied by using cyclic and differential-pulse voltammetric methods. The redox potentials of these materials are listed in Table 1. The cyclic voltammograms for **4**, **16**, **7**, and NPB are shown in Figure 2. Except for **16**, all compounds exhibit two reversible one-electron redox processes, indicating that the two peripheral arylamines at the 2 and 7 positions of the carbazole core are electronically coupled. The two peripheral amines of compound **16** are oxidized simultaneously. Apparently, the distance between the two amines is too long to allow electronic communication between them. These arguments are supported by Osteryoung square-wave voltammetry (Fig. 2a and b, insets). A comparison of the first oxidation potentials of **7** (+125 mV) and NPB (+314 mV) clearly indicates that the planar biphenyl unit of the central carbazole in the

ADVANCED FUNCTIONAL MATERIALS

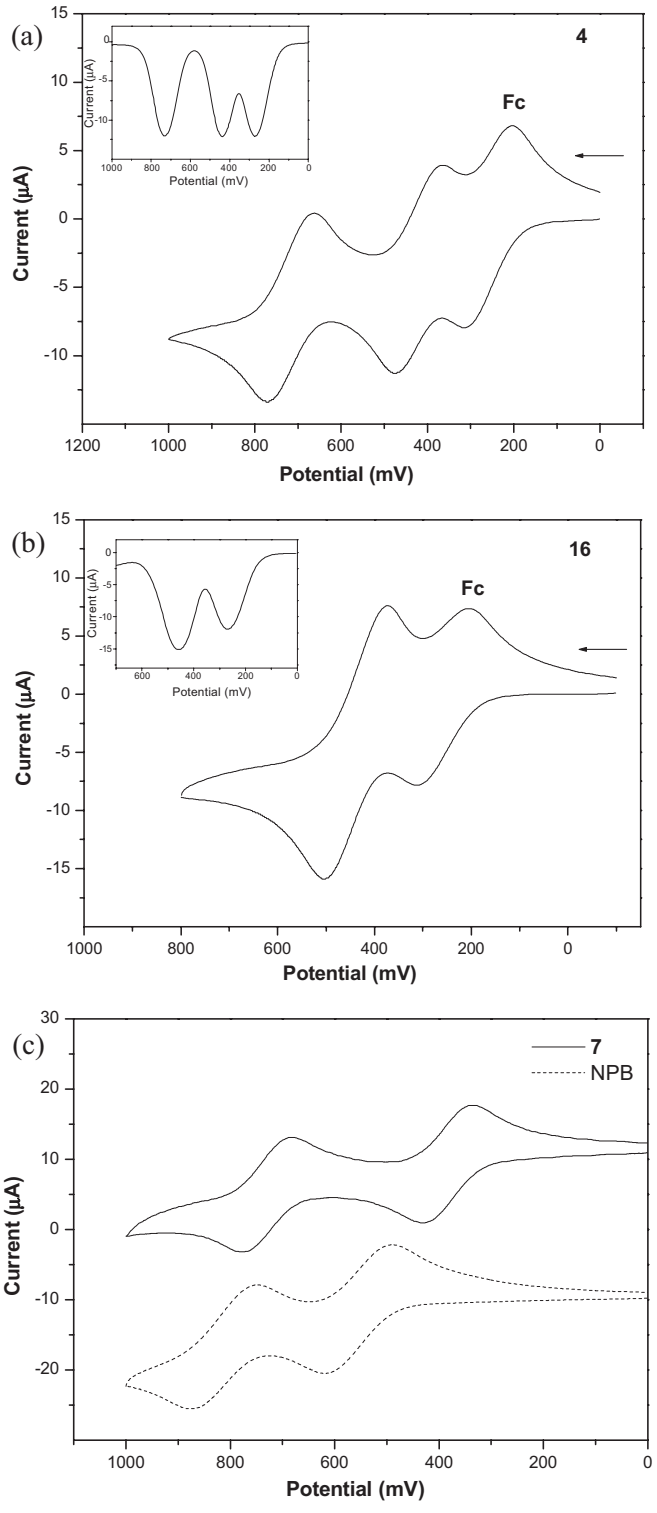

Figure 2. a–c) Cyclic voltammograms of compounds **4** (a), **16** (b), **7** and NPB (without ferrocene) (c), measured in dichloromethane.

former is beneficial to the electronic communication between the two peripheral amines. The larger difference between the first and second oxidation potential in **7** (+346 mV) compared to NPB (+258 mV) further supports this argument. The interaction between the two peripheral amines through the central biphenyl unit is expected to be stronger in 2,7-disubstituted carbazoles than in 3,6-disubstituted carbazoles, if the role of the carbazolyl nitrogen atom is overlooked. However, we found that the first oxidation potential of **7** (+125 mV) is very similar to that of its analogue **7A** (+127 mV),[7a] and that the value for **9** (+119 mV) is similar to **9A** (+116 mV).[7a] Obviously, the carbazolyl nitrogen atom interacts strongly with both of the peripheral amines in the 3,6-disubstituted carbazole because the former is at the para position to the latter in the same phenyl ring.

The presence of the electron-withdrawing cyano group in **6** and the oxadiazole unit in **15** results in a significant anodic shift of the potential. The presence of the cyano group also results in a higher first oxidation potential for **13** (+25 mV) compared to **11** (–21 mV). It is interesting to note that **11** and **13** have very low first oxidation potentials because of the electron-donating nature of the peripheral 3-carbazolyl groups. The third oxidation wave for **3** and **8**–**11** is attributable to the oxidation of the central carbazole[7a] or to the oxidation of peripheral segments, such as anthracene, pyrene, and carbazole. This oxidation is irreversible, with the exception of **11**. Evidently, the electron-donating 3-carbazolyl peripheral groups in **11** help to stabilize the trivalent cation and lead to reversibility as well as an anodic shift of the third oxidation potential compared to other compounds. The fourth irreversible oxidation in **11** may be a result of the polymerization of the central carbazole at the 3 and 6 positions after oxidation.[10c,e]

2.4. Optical Properties

The absorption and luminescence spectra of the compounds were measured in dichloromethane, and the pertinent data are presented in Table 1. Representative absorption spectra are shown in Figure 3. The absorptions that fall within $\lambda_{max} = 300$–444 nm are attributed to $n \rightarrow \pi^*$ and $\pi \rightarrow \pi^*$ transitions. An-

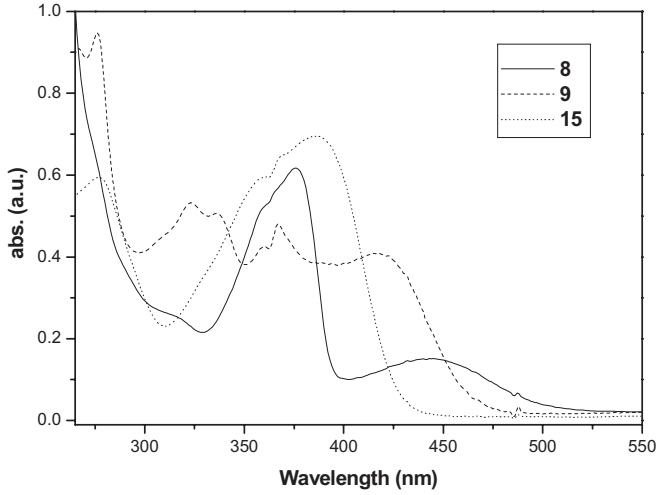

Figure 3. Absorption spectra of compounds **8**, **9**, and **15** in dichloromethane.

thracene- or pyrene-containing compounds display a distinct absorption at longer wavelengths, which may be assigned to localized *N*-anthracene and *N*-pyrene $\pi \rightarrow \pi^*$ transitions. Only **1**, **4**, and **12** have a fluorescence quantum yield greater than 0.5 in dichloromethane. Similar to the 3,6-disubstituted carbazolyl analogues we reported earlier,[7a] this behavior is likely a result of reductive quenching by the amines. The emission colors of the compounds range from orange to purple blue. Among these, compound **8**, containing anthracene, has the most red-shifted emission in dichloromethane or toluene. Except for **1**, **4**, **11**, and **12** ($\lambda(CH_2Cl_2) - \lambda(\text{toluene}) < 3$ nm), the emission wavelengths are very sensitive to the solvent polarity, indicating the dipolar nature of the excited-state compounds. Compounds **7** and **9** appear to have longer absorption wavelengths than **7A** and **9A** in both CH_2Cl_2 (Table 1) and toluene (λ_{max}: **7**, 373 nm; **7A**, 357 nm; **9**, 422 nm; **9A**, 414 nm). This trend seems to be consistent with the increased delocalized nature of the 2,7-substituted carbazoles compared to the 3,6-substituted analogues. It is noteworthy that the 2,7-disubstituted carbazole compounds have a larger molar absorptivity than the 3,6-disubstituted compounds (ε_{max} in toluene: **7**, 38 361 $M^{-1}\,cm^{-1}$; **7A**, 16 717 $M^{-1}\,cm^{-1}$; **9**, 61 149 $M^{-1}\,cm^{-1}$; **9A**, 35 655 $M^{-1}\,cm^{-1}$).

2.5. Charge-Transport Properties

Carrier-transport properties of **7** and **9** were investigated by the time-of-flight (TOF) transient photocurrent technique in vacuum at room temperature. Their 3,6-disubstituted counterparts **7A** and **9A** were also subjected to measurement for comparison. Representative TOF transients for holes and electrons of **7** are shown in Figure 4a and b, respectively, while representative hole and electron signals of **9** are shown in Figure 4c and d, respectively. Similarly, representative TOF transients for **7A** and **9A** are shown in Figure 4e–h. While the hole transport for **7** and **9A** is nondispersive, that for **9** and **7A** is dispersive. On the other hand, the electron transport is dispersive for all investigated compounds. The carrier-transit times (t_T) needed for determining carrier mobilities were evaluated from the intersection points of two asymptotes from the double-logarithmic plots (Fig. 4, insets). The obtained carrier mobilities are shown as a function of the square root of the electric field ($E^{1/2}$) in Figure 5. The field dependence of the carrier mobilities follows the nearly universal Poole–Frenkel relationship: $\mu \propto \exp(\beta E^{1/2})$, as usually observed for disordered organic systems, where β is the Poole–Frenkel factor.[20]

The hole mobilities of the 2,7-disubstituted carbazole compounds are one to two orders of magnitude higher than those of the 3,6-disubstituted congeners, i.e., **7** (ca. 10^{-4} $cm^2\,V^{-1}\,s^{-1}$) > **7A** ($2–3 \times 10^{-6}$ $cm^2\,V^{-1}\,s^{-1}$) and **9** (ca. 6×10^{-4} $cm^2\,V^{-1}\,s^{-1}$) > **9A** ($10^{-4}–10^{-5}$ $cm^2\,V^{-1}\,s^{-1}$). Some of the hole mobilities are comparable to those of NPB (ca. 10^{-3} $cm^2\,V^{-1}\,s^{-1}$).[21] The relatively high electron mobilities observed for 2,7-disubstituted carbazoles (**7**, ca. 10^{-4} $cm^2\,V^{-1}\,s^{-1}$; **9**, ca. 2×10^{-4} $cm^2\,V^{-1}\,s^{-1}$) and 3,6-disubstituted carbazoles (**7A**, $4–6 \times 10^{-5}$ $cm^2\,V^{-1}\,s^{-1}$; **9A**, ca. 10^{-4} $cm^2\,V^{-1}\,s^{-1}$) are somewhat unexpected because arylamines are normally viewed as hole-transporting materials.[1a] However, we note that some carbazole derivatives were previously reported to show electron transport. For instance, carbazoles with cyano substituents were reported to be capable of electron-transport.[22] Furthermore, 4,4′-*N*,*N*′-dicarbazole-biphenyl (CBP) has also been demonstrated to be an ambipolar conductive material.[23] Still, the electron mobilities reported here appear to be high compared to common electron-transport materials such as 1,3,5-tris(*N*-phenylbenzimidazol-2-yl)benzene (TPBI) and tris(8-hydroxyquinoline)aluminum (Alq_3).[24] When comparing (either hole or electron) carrier-transport properties of 2,7- and 3,6-disubstituted carbazoles, it is interesting to note that in general 2,7-disubstituted compounds show higher mobilities than 3,6-disubstituted carbazoles. The more extended conjugation network in 2,7-disubstituted carbazoles may result in stronger electronic coupling between molecules, thereby facilitating carrier hopping. It is also possible that the very different linking topologies (and thus conformations) in 2,7- and 3,6-disubstituted carbazoles lead to significant differences in molecular packing, which in turn affects the molecular packing density and the positional disorder in thin films, which are critical for carrier transport.

2.6. Electroluminescence Properties

The highest occupied molecular orbital (HOMO) energy levels of the compounds were calculated from cyclic voltammetry (Section 2.5) and by comparison with ferrocene (4.8 eV).[25] These data, together with absorption spectra, were used to determine the lowest unoccupied molecular orbital (LUMO) energy levels (Table 1, Fig. 6). According to the obtained HOMO and LUMO energy levels, the compounds in this study appear to be good candidates for hole-transporting and emitting materials (see below).

Compounds with high solution quantum yields were used to fabricate two types of double-layered devices, using TPBI (HOMO = 6.2 eV; LUMO = 2.7 eV)[26] or Alq_3 (HOMO = 6.0 eV; LUMO = 3.3 eV)[27] as electron-transport materials. Type I devices consisted of indium tin oxide (ITO)/2,7-carb (40 nm)/TPBI (40 nm)/Mg:Ag, while type II devices comprised ITO/2,7-carb (40 nm)/Alq_3 (40 nm)/Mg:Ag. The performance characteristics of all devices are summarized in Table 2. Representative voltage–current density (*V*–*J*) characteristics of the type I and type II devices are shown in Figure 7a and b, respectively, while representative current–luminance (*I*–*L*) characteristics are shown in Figure 8a and b, respectively. Figure 9 shows the electroluminescence (EL) spectra of some type I and type II devices. All devices in this study exhibited relatively low turn-on voltages (2.4–3.0 V), perhaps because of the small energy difference between the work function of ITO and the HOMO levels of the 2,7-disubstituted carbazoles. In the type I devices, with TPBI as the electron-transporting layer (ETL), blue to green light was emitted from the 2,7-disubstituted carbazole compounds. It is conceivable that TPBI serves as an effective hole blocker because of the large HOMO energy gap (1.12–1.42 eV) between TPBI and the 2,7-disubstituted carbazoles. In contrast, the relatively smaller LUMO energy gap (0.37–0.87 eV) between TPBI and 2,7-disubstituted compounds facilitates injection of the electrons from TPBI into the organic-

ADVANCED FUNCTIONAL MATERIALS

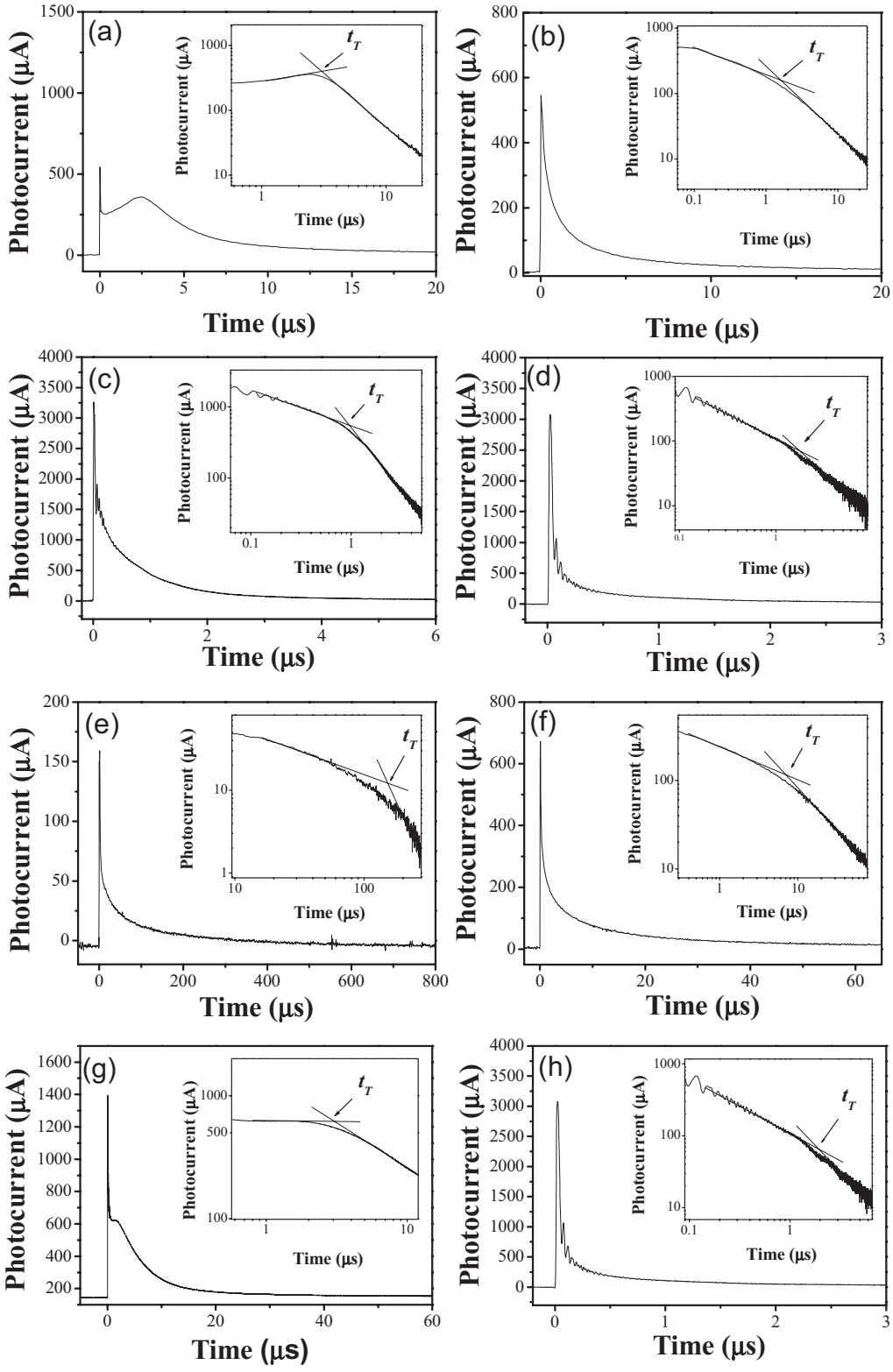

Figure 4. Time-of-flight (TOF) transients for 2,7-carb (2.0 μm thick): a) **7**, hole, $E = 3.5 \times 10^5$ V cm^{-1}. b) **7**, electron, $E = 3.5 \times 10^5$ V cm^{-1}. c) **9**, hole, $E = 3.5 \times 10^5$ V cm^{-1}. d) **9**, electron, $E = 4.5 \times 10^5$ V cm^{-1}. e) **7A**, hole, $E = 3.5 \times 10^5$ V cm^{-1}. f) **7A**, electron, $E = 3.5 \times 10^5$ V cm^{-1}. g) **9A**, hole, $E = 4.5 \times 10^5$ V cm^{-1}. h) **9A**, electron, $E = 3.5 \times 10^5$ V cm^{-1}.

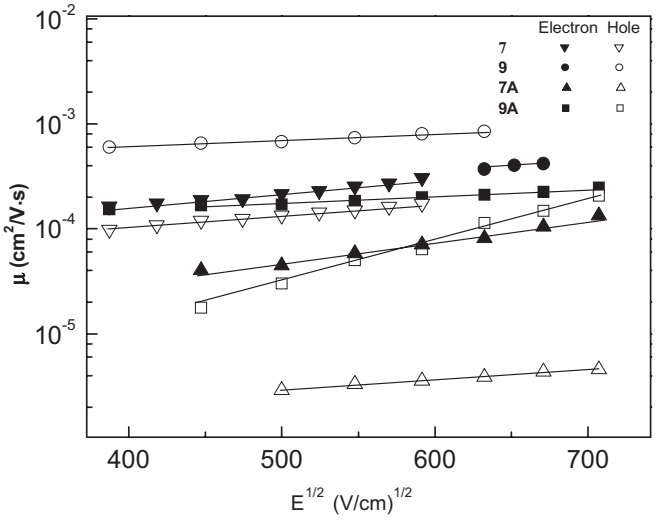

Figure 5. Electron and hole mobilities versus $E^{1/2}$ for **7**, **9**, **7A**, and **9A**.

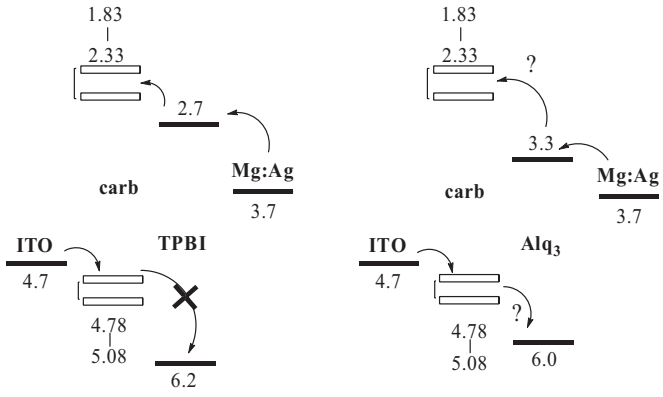

Figure 6. Relative energy alignments of the materials in type I (left) and type II (right) devices.

compound layer. In type II devices, with Alq_3 as ETL, the emission was also found to be from the 2,7-disubstituted carbazole layer for **3**, **9**, **10**, and **16**. All others emitted green light characteristic of Alq_3 (bandwidth > 92 nm).

It is believed that the LUMO energy offset between the HTL and ETL materials is critical for the transport and distribution of electrons, which in turn would determine the carrier-recombination (emission) zone. Among series of compounds used for device fabrication, **3**, **9**, **10**, and **16** have lower-lying LUMO levels (2.24–2.33 eV), and thus smaller energy barriers for electron injection from the ETL, than others (LUMO = 1.83–1.91 eV, except for **15**: 2.17 eV). The larger LUMO energy offset is thought to effectively block the injection of electrons from the ETL into the HTL, thus confining electrons and carrier recombination mainly to the ETL. This is consistent with our previous observations on devices based on 3,6-disubstituted carbazoles.[7a] Interestingly, for the type II device of **15**, emission from both the HTL and the ETL (Alq_3) was observed, suggesting exciton formation in both layers. This may be because the barrier at the HTL/ETL does not completely block electron injection into the HTL, and also because the oxadiazolyl moieties decrease the hole mobility of **15** and retard hole transport into the ETL.

The luminescence wavelength of the carbazole compounds in this study can be tuned from green to blue by modification

Table 2. Electroluminescence data for the type I and type II devices.

Compound	V_{on} [V]	L_{max} (V at L_{max}) [cd m^{-2} (V)]	λ_{em} [nm]	CIE [x,y]	FWHM [nm]	$\eta_{ext,max}$ [%]	$\eta_{p,max}$ [lm W^{-1}]	$\eta_{c,max}$ [cd A^{-1}]	L [a] [cd m^{-2}]	η_{ext} [a] [%]	η_p [a] [lm W^{-1}]	η_c [a] [cd A^{-1}]
2	2.8; 3.0	12919 (11.5); 22138 (15.0)	478; 524	0.15, 0.26; 0.31, 0.56	74; 96	1.0; 1.4	1.1; 2.0	1.8; 2.7	1788; 2696	1.0; 0.83	1.0; 1.2	1. 8; 2.7
3	2.8; 2.8	36514 (12.0); 28952 (12.0)	530; 532	0.33, 0.61; 0.34, 0.60	78; 78	1.6; 2.3	5.3; 5.6	5.6; 5.0	5411;4684	1.5; 1.3	2.8; 2.0	5.4; 4.7
7	2.8; 3.0	21147 (13.0); 32192 (15.0)	470; 524	0.15, 0.20; 0.31, 0.56	70; 92	1.9; 1.7	2.1; 2.6	2.5; 3.8	2809; 3757	1.6; 1.2	1.6; 1.8	2.5; 3.8
9	2.6; 2.5	58120 (13.0); 42250 (13.5)	520; 522	0.28, 0.60; 0.28, 0.60;	76; 76	2.4; 1.8	6.6; 4.5	8.1; 6.1	7672; 5779	2.3; 1.7	3.4; 2.9	7.7; 5.8
10	2.7; 2.7	56060 (13.0); 39702 (13.5)	538; 538	0.34, 0.61; 0.35, 0.60	68; 70	3.2; 2.2	6.88; 5.03	9.85; 8.0	8868; 7152	2.4; 1.9	4.9; 3.0	8.9; 7.2
11	2.5; 3.0	3188 (12.0); 7904 (14.0)	442; 528	0.18, 0.18; 0.33, 0.55	60; 104	0.41; 0.34	0.50; 0.54	0.61; 1.09	587; 1067	0.40; 0.33	0.31; 0.46	0.59; 1.1
13	2.4; 3.0	28120 (14.5); 21319 (15)	508; 526	0.24, 0.46; 0.32, 0.55	96; 96	1.7; 0.80	4.0; 1.2	4.7; 2.6	4270; 2548	1.6; 0.79	2.2; 1.1	4.3; 2.5
15	2.7; 3.0	15300 (13.5); 12506 (15)	486; 502	0.20, 0.37; 0.24, 0.43	88; 102	2.6; 1.4	5.4; 3.5	6.0; 3.9	5104; 3334	2.2; 1.3	2.1; 1.1	5.1; 3.3
16	2.75; 3.0	13747 (15); 13154 (15)	508; 512	0.26, 0.53; 0.28, 0.55	88; 90	0.81; 0.73	1.5; 1.4	2.43; 2.26	1983; 2077	0.66; 0.67	1.0; 0.91	2.0; 2.1

[a] Measured at a current density of 100 mA cm^{-2}. The measured values are given in order of the type I (TPBI) and type II (Alq_3) devices. V_{on} was obtained from the x-intercept of log(luminance) versus applied voltage plot. L_{max}: maximum luminance; L: luminance; V_{on}: turn-on voltage; CIE: Commision Internationale de l'Eclairage; V: voltage; $\eta_{ext,max}$: maximum external quantum efficiency; $\eta_{p,max}$: maximum power efficiency; $\eta_{c,max}$: maximum current efficiency; η_{ext}: external quantum efficiency; η_p: power efficiency; η_c: current efficiency; FWHM: full width at half-maximum.

ADVANCED FUNCTIONAL MATERIALS

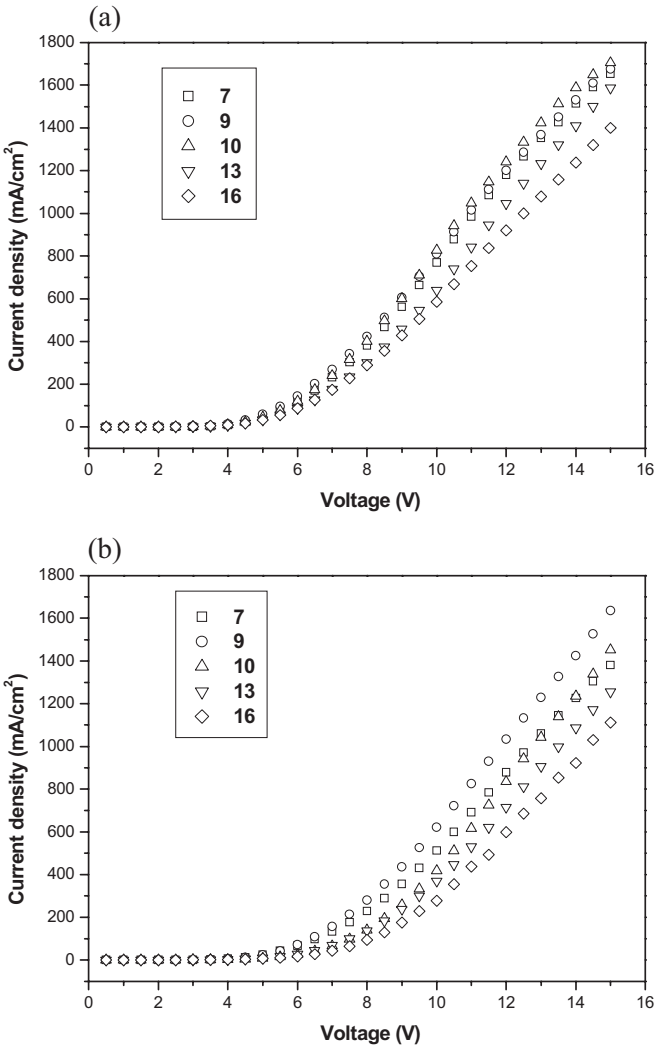

Figure 7. Current density versus applied electric voltage characteristics of type I (a) and type II (b) devices.

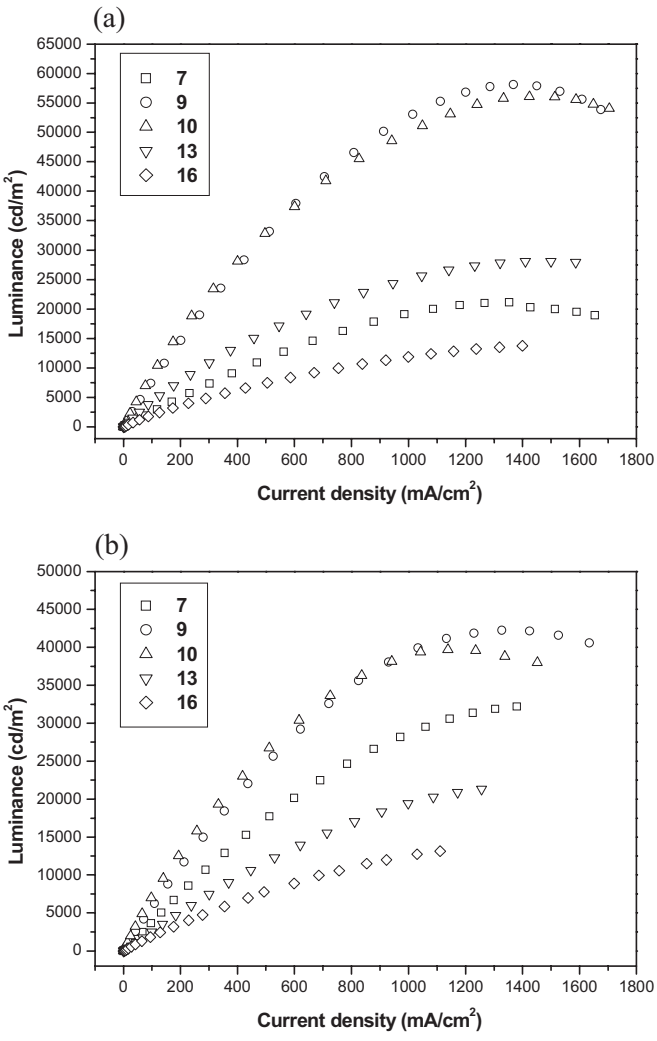

Figure 8. Luminance versus current density characteristics of type I (a) and type II (b) devices.

of the peripheral group. As the devices are not optimized, the performances of the green-emitting type I and type II devices fabricated from **3**, **9**, and **10** appear to be promising: maximum luminescence 28 952–58 120 cd m^{-2}, maximum external quantum efficiency 1.6–3.2 %, and maximum luminous efficiency 4.47–6.88 lm W^{-1}. Their performances surpass the standard green-emitting device; ITO/NPB (50 nm)/Alq_3 (50 nm)/Mg:Ag (L = 3629 cd m^{-2}; η_{ext} = 1.2 %; η_p = 1.2 lm W^{-1} at 100 mA cm^{-2}). Among blue emitting devices, those of **7** and **15** have the best performance (**7**: L = 2809 cd m^{-2}, $\eta_{ext,max}$ = 1.6 %, η_c = 2.5 cd A^{-1}, η_p = 1.6 lm W^{-1} at 100 mA cm^{-2}; **15**: L = 5104 cd m^{-2}, $\eta_{ext,max}$ = 2.2 %, η_c = 5.1 cd A^{-1}, η_p = 2.1 lm W^{-1} at 100 mA cm^{-2}).

It is interesting to note that both type I and type II devices of **7** and **9** have better performance characteristics than corresponding devices prepared from their 3,6-disubstituted carbazole counterparts.[7a] The better emission performance of the type I device incorporating **7** compared to **7A** may be rationalized by the better electron-transport properties and higher

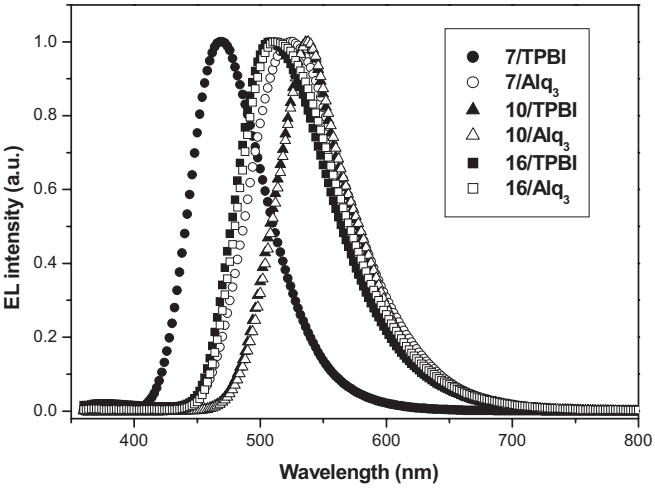

Figure 9. EL spectra of the type I and type II devices for selected compounds.

quantum yield of **7** (thin-film quantum yields: **7**, 21 %; **7A**, 15 %). In the type II devices (emission from Alq_3), the formation of excitons in Alq_3 is perhaps less efficient for **7A** than for **7** because of the much lower hole mobility of **7A**. Similarly, the better performances of the type I and type II devices for **9** (emission from **9** in both) than for **9A** are possibly associated with better electron transport in **9** (film quantum yield: **9**, 32 %; **9A**, 42 %). A comparison is also made between the compounds in this study and compounds with a similar carbon skeleton: 2,7-carbazole derivatives without arylamines, 4,4′-bis(diarylamine)-biphenyl, and 2,7-bis(diarylamino)-9,9-dimethylfluorene. Although compound **7** has a lower solution quantum yield ($\Phi = 0.25$ in toluene) than 2,7-bis(2,2-diphenylvinyl)-9-isopropyl-9*H*-carbazole ($\Phi = 0.37$ in toluene) and 2,7-bis(2,2-diphenylvinyl)-9-tolyl-9*H*-carbazole ($\Phi = 0.51$ in toluene),[28] the type I device for **7** has a much better performance than the devices of similar structure for the other two. It is possible that the presence of the two peripheral arylamines in **7** results in a smaller energy gap between the Fermi level of ITO and the HOMO of **7**, and in a better balance of carriers mobilities. When used as the hole-transport layer in devices, type II devices for **2** and **7** have performances comparable to the device using NPB (see above) as the hole-transport layer. In contrast, the performances of the type II devices for **2** and **7**, on the other hand, appear to be better than that of the device from 2,7-bis(diarylamino)-9,9-dimethylfluorene, using 2,7-bis(diarylamino)-9,9-dimethylfluorene/polystyrene blend (with hole mobility $< 10^{-4}$ $cm^2 V^{-1} s^{-1}$) as the hole-transporting layer.[29]

3. Conclusions

We have synthesized a series of 2,7-carbazole derivatives containing arylamines via palladium-catalyzed C–N and Stille C–C coupling reactions. The new compounds possess high glass transition temperatures and can function as emitting and/or hole-transporting materials. The two peripheral arylamines are electronically coupled through the biphenyl spacer in these 2,7-disubstituted carbazole compounds. This is in contrast to their 3,6-disubstituted carbazole congeners, in which the two peripheral arylamines are coupled via the nitrogen atom of the central carbozolyl unit. It is intriguing that the 2,7-disubstituted compounds exhibit somewhat ambipolar conductive behavior, and have higher and more balanced electron and hole mobilities than their 3,6-disubstituted analogues. Double-layer devices using the compounds either as the hole-transporting materials or as the emitting materials exhibit promising performances. Further modification of the molecules at the 2-, 7-, and 9-positions of carbazole aimed at color tuning and introducing multiple functions is ongoing.

4. Experimental

4.1 General Information

Unless otherwise specified, all reactions were carried out under a nitrogen atmosphere using standard Schlenk techniques. Solvents were dried by standard procedures. Column chromatography was performed with silica gel (230–400 mesh, Macherey–Nagel GmbH & Co.) as the stationary phase. ^{1}H NMR spectra were recorded on a Bruker AMX400 spectrometer. Electronic absorption spectra were measured in dichloromethane using a Cary 50 Probe UV-visible spectrophotometer. Emission spectra were recorded by a Hitachi F-4500 fluorescence spectrometer. Emission quantum yields were measured with reference to coumarin 1 or coumarin 6 in CH_3CN [30]. Cyclic voltammetry experiments were performed with a BAS-100 electrochemical analyzer. All measurements were carried out at room temperature with a conventional three-electrode configuration consisting of platinum working and auxiliary electrodes and a nonaqueous $Ag/AgNO_3$ reference electrode. The $E_{1/2}$ values were determined as $1/2(E_p^a + E_p^c)$, where ^a_p and ^c_p are the anodic and cathodic peak potentials, respectively. The solvent in all experiments was CH_2Cl_2, and the supporting electrolyte was 0.1 M tetrabutylammonium perchlorate. DSC measurements were carried out using a Perkin–Elmer 7 series thermal analyzer at a heating rate of 10 °C min^{-1}. TGA measurements were performed on a Perkin–Elmer TGA7 thermal analyzer. Mass spectra (FAB) were recorded on a JMS-700 double focusing mass spectrometer (JEOL, Tokyo, Japan). Elementary analyses were performed on a Perkin–Elmer 2400 CHN analyzer. Compounds 2,7-dibromo-9*H*-carbazole [11], (9-ethyl-9*H*-carbazole-3-yl)-phenyl-amine [7c], 5-[*N*,*N*-diphenylamino]-2-(tri-*n*-butylstannyl)-thiophene [31], [(2′,7′-di-*tert*-butyl)-9,9′-spirobifluoren-2-yl]-phenyl-amine [15], 9-ethyl-6-(naphthalen-1-ylamino)-9*H*-carbazole-3-carbonitrile [15], 9-ethyl-*N*,*N*′-diphenyl-9*H*-carbazole-2,7-diamine (**14**) [32], and *N*,*N*′-bis-{4-[5-(4-*tert*-butyl-phenyl)-[1,3,4]oxadiazol-2-yl]-phenyl}-9-ethyl-*N*,*N*′-diphenyl-9*H*-carbazole-2,7-diamine (**15**) [32] were prepared according to published procedures.

4.2 Synthesis Details

*4.2.1 General Procedure A for the Synthesis of Compound **1**–**3***

The corresponding 4,4′-dibromo-2-nitro-biphenyl (1.5 mmol), secondary amine (3.2 mmol), $Pd(OAc)_2$ (15 mg, 0.06 mmol), $(t\text{-}Bu)_3P$ (0.06 mmol), sodium *tert*-butoxide (0.43 g, 4.5 mmol) and toluene (30 mL) were charged in a two-necked flask kept under nitrogen. The mixture was heated at reflux for 48 h. After cooling, the solvent was removed under vacuum and the residue was extracted with dichloromethane/water. The organic layer was dried over $MgSO_4$ and filtered. The filtrate was pumped dry to afford the crude compound, 4,4′-bis(diarylamino)-2-nitrobiphenyl. A mixture of the crude 4,4′-bis(diarylamino)-2-nitrobiphenyl and triethyl phosphite (10 mL) was heated at reflux for 24 h in an inert atmosphere. Excess triethyl phosphite was removed by distillation and the residue was extracted with dichloromethane/water. The organic layer was dried over $MgSO_4$ and filtered. The residue obtained after evaporation of the solvent was chromatographed on silica gel using dichloromethane/hexanes mixture as eluent.

N,N,N′,N′-*Tetraphenyl-9*H-*carbazole-2,7-diamine* (***1***): White solid. Yield: 43 %. Fast atom bombardment (FAB) mass spectrometry (MS): *m/z* 501 (M^+). ^{1}H NMR (acetone-d_6, δ): 10.01 (s, 1H, N*H*), 7.94 (d, $J = 8.3$ Hz, 2H, C_6H_3), 7.27 (d, $J = 7.4$ Hz, 8H, *meta*-C_6H_5), 7.11–7.07 (m, 10H, *ortho*-C_6H_5 and C_6H_3), 7.00 (t, $J = 7.4$ Hz, 4H, *para*-C_6H_5), 6.91 (d, $J = 7.4$ Hz, 2H, C_6H_3). Anal. Calcd for $C_{36}H_{27}N_3$: C 86.20, H 5.43, N 8.38; found: C 85.96, H 5.13, N 8.11.

N,N′-*Di-naphthalen-1-yl*-N,N′-*diphenyl-9*H-*carbazole-2,7-diamine* (***2***): Yellow solid. Yield: 34 %. FAB MS: *m/z* 601 (M^+). ^{1}H NMR (acetone-d_6, δ): 9.78 (s, 1H, NH), 8.01–7.95 (m, 4H, $C_{10}H_7$), 7.87–7.84 (m, 4H, $C_{10}H_7$ and C_6H_3), 7.53 (t, $J = 7.4$ Hz, 2H, $C_{10}H_7$), 7.47 (t, $J = 7.4$ Hz, 2H, $C_{10}H_7$), 7.35–7.34 (m, 4H, $C_{10}H_7$), 7.20 (t, $J = 7.4$ Hz, 4H, *meta*-C_6H_5), 6.99–6.83 (m, 10H, *ortho*-, *para*-C_6H_5 and C_6H_3). Anal. Calcd for $C_{44}H_{31}N_3$: C 87.82, H 5.19, N 6.98; found: C 87.74, H 4.91, N 6.69.

N,N′-*Diphenyl*-N,N′-*di-pyren-1-yl-9*H-*carbazole-2,7-diamine* (***3***): Yellow solid. Yield: 40 %. FAB MS: *m/z* 749 (M^+). ^{1}H NMR (acetone-d_6, δ): 9.76 (s, 1H, N*H*), 8.30–8.25 (m, 4H, pyrenyl), 8.23–8.12 (m, 8H, pyrenyl), 8.05–7.98 (m, 4H, pyrenyl and C_6H_3), 7.90–7.88 (m, 4H, pyrenyl), 7.22 (t, $J = 7.6$ Hz, 4H, *meta*-C_6H_5), 7.05 (d, $J = 7.6$ Hz, 4H, *ortho*-C_6H_5), 6.98–6.92 (m, 6H, *para*-C_6H_5 and C_6H_3). Anal. Calcd for $C_{56}H_{35}N_3$: C 89.69, H 4.70, N 5.60; found: C 89.28, H 4.90, N 5.33.

4.2.2. 9-(4-tert-Butyl-phenyl)-N,N,N′,N′-tetraphenyl-9H-carbazole-2,7-diamine (**4**)

A mixture of 1-bromo-4-*tert*-butylbenzene (1 mmol), compound **1** (1 mmol), ground K_2CO_3 (1.2 mmol), Cu powder (0.3 mmol), and nitrobenzene (5 mL) was heated at reflux for 72 h. After cooling, the solvent was removed under vacuum and the residue was extracted with dichloromethane/water. The organic layer was dried over $MgSO_4$ and filtered. The residue obtained after evaporation of the solvent was chromatographed through silica gel using dichloromethane/hexanes mixture as eluent. Compound **4** was obtained as a white solid in 75 % yield. FAB MS: *m/z* 633 (M^+). ^{1}H NMR (acetone-d_6, δ): 8.06 (d, J = 8.3 Hz, 2H, C_6H_3), 7.52 (d, J = 8.6 Hz, 2H, C_6H_4), 7.39 (d, J = 8.6 Hz, 2H, C_6H_4), 7.25 (t, J = 7.8 Hz, 8H, *meta*-C_6H_5), 7.07 (t, J = 7.8 Hz, 10H, C_6H_3 and *ortho*-C_6H_5), 6.98 (t, J = 7.2 Hz, 6H, *para*-C_6H_5 and C_6H_3), 1.28 (s, 9H, CH_3). Anal. Calcd for $C_{46}H_{39}N_3$: C 87.17, H 6.20, N 6.63; found: C 86.79, H 6.06, N 6.67.

4.2.3 2,7-Dibromo-9-ethyl-9H-carbazole (**5**)

Bromoethane (1.63 g, 15 mmol) was added dropwise to a flask containing a mixture of 2,7-dibromocarbazole (3.22 g, 10.0 mmol), aqueous 50 % sodium hydroxide (10 mL), benzene (5 mL), and BTEAC (0.55 mg, 0.3 mmol). The reaction was continued at room temperature for 4 h. The reaction mixture was poured into hot water and left overnight at room temperature. The precipitated solid was collected, washed with water and dried. Recrystallizations from ethanol afforded **5** as a white powder in 90 % yield (3.15 g). FAB MS: *m/z* 350 (M^+). ^{1}H NMR (acetone-d_6, δ): 8.09 (d, J = 8.3 Hz, 2 H, *H*-4 of C_6H_3), 7.82 (s, 2 H, *H*-1 of C_6H_3), 7.36 (d, J = 8.3 Hz, 2 H, *H*-3 of C_6H_3), 4.51 (q, J = 7.1 Hz, 2 H, CH_2), 1.41 (t, J = 7.1 Hz, 3H, CH_3). Anal. Calcd for $C_{14}H_{11}Br_2N$: C 47.63, H 3.14, N 3.97; found: C 47.51, H 2.93, N 3.53

4.2.4. General Procedure B for the Synthesis of Compound **6–13**

The corresponding compound **5** (1.5 mmol), secondary amine or aniline (3.2 mmol), $Pd(OAc)_2$ (15 mg, 0.06 mmol), (t-Bu)$_3$P (0.06 mmol), sodium *tert*-butoxide (0.43 g, 4.5 mmol) and toluene (30 mL) were charged in a two-necked flask kept under nitrogen. The mixture was heated at reflux for 48 h. After cooling, the solvent was removed under vacuum and the residue was extracted with dichloromethane/water. The organic layer was dried over $MgSO_4$ and filtered. The residue obtained after evaporation of the solvent was chromatographed through silica gel using dichloromethane/hexanes mixture as eluent.

*2,7-bis[(*N*-phenyl)-4-cyanophenylamino]-9-ethyl-9*H*-carbazole* (**6**): Pale yellow solid. Yield: 82 %. FAB MS: *m/z* 579 (M^+). ^{1}H NMR (acetone-d_6, δ): 8.15 (d, J = 8.2 Hz, 2H, *H*-4 of C_6H_3), 7.53 (d, J = 8.8 Hz, 4H, C_6H_4), 7.47 (d, J = 1.4 Hz, 2H, *H*-1 of C_6H_3), 7.41 (t, J = 7.8 Hz, 4H, *meta*-C_6H_5), 7.29 (d, J = 7.8 Hz, 4H, *ortho*-C_6H_5), 7.22 (t, J = 7.8 Hz, 2H, *para*-C_6H_5), 7.05 (dd, J = 8.2, 1.6 Hz, 2H, *H*-3 of C_6H_3), 7.01 (d, J = 8.8 Hz, 4H, C_6H_4), 4.32 (q, J = 7.1 Hz, 2H, CH_2), 1.26 (t, J = 7.1 Hz, 3H, CH_3). Anal. Calcd for $C_{40}H_{29}N_5$: C 82.88, H 5.04, N 12.08; found: C 82.75, H 4.93, N 11.83

9-Ethyl-N,N′-*di-naphthalen-1-yl*-N,N′-*diphenyl-9*H-*carbazole-2,7-diamine* (**7**): Yellow solid. Yield: 75 %. FAB MS: *m/z* 629 (M^+). ^{1}H NMR ($CDCl_3$, δ): 8.00 (d, J = 8.3 Hz, 2H, $C_{10}H_7$), 7.96 (d, J = 8.3 Hz, 2H, $C_{10}H_7$), 7.85 (m, 4H, $C_{10}H_7$), 7.52 (t, J = 8.3 Hz, 2H, $C_{10}H_7$), 7.47 (t, J = 8.2 Hz, 2H, $C_{10}H_7$), 7.37 (m, 4H, $C_{10}H_7$ and C_6H_3), 7.21 (t, J = 8.2 Hz, 4H, *meta*-C_6H_5), 7.14 (s, 2H, C_6H_3), 6.98–6.90 (m, 8H, *para*-, *ortho*-C_6H_5 and C_6H_3), 4.00 (q, J = 7.2 Hz, 2H, CH_2), 1.05 (t, J = 7.2 Hz, 3H, CH_3). Anal. Calcd for $C_{46}H_{35}N_3$: C 87.73, H 5.60, N 6.67; found: C 87.28, H 5.32, N 6.38.

N,N′-*Di-anthracen-9-yl-9-ethyl*-N,N′-*diphenyl-9*H-*carbazole-2,7-diamine* (**8**): Yellow solid. Yield: 80 %. FAB MS: *m/z* 729 (M^+). ^{1}H NMR ($CDCl_3$, δ): 8.47 (s, 2H, anthracenyl), 8.15 (d, J = 8.4 Hz, 4H, anthracenyl), 8.02 (d, J = 8.4 Hz, 4H, anthracenyl), 7.60 (d, J = 8.2 Hz, 2H, C_6H_3), 7.40 (t, J = 7.6 Hz, 4H, anthracenyl), 7.31 (t, J = 8.0 Hz, 4H, anthracenyl), 7.14–7.03 (m, 10H, C_6H_3 and C_6H_5), 6.84–6.79 (m, 4H, C_6H_3 and *para*-C_6H_5), 3.83 (q, J = 7.0 Hz, 2H, CH_2), 1.05 (t, J = 7.0 Hz, 3H, CH_3). Anal. Calcd for $C_{54}H_{39}N_3$: C 88.86, H 5.39, N 5.76; found: C 88.40, H 5.27, N 5.47.

9-Ethyl-N,N′-*diphenyl*-N,N′-*di-pyren-1-yl-9*H-*carbazole-2,7-diamine* (**9**): Yellow solid. Yield: 86 %. FAB MS: *m/z* 777 (M^+). ^{1}H NMR (acetone-d_6, δ): 8.31–8.13 (m, 12H, pyrenyl), 8.06–7.99 (m, 4H, pyrenyl), 7.91–7.89 m, 4H, pyrenyl and C_6H_3), 7.25–7.21 (t, J = 7.6 Hz, 6H, *meta*-C_6H_5 and C_6H_3), 7.05 (d, J = 7.6 Hz, 4H, *ortho*-C_6H_5), 6.96–6.93 (m, 4H, *para*-C_6H_5 and C_6H_3), 3.99 (q, J = 7.0 Hz, 2H, CH_2), 1.02 (t, J = 7.0 Hz, 3H, CH_3). Anal. Calcd for $C_{58}H_{39}N_3$: C 89.55, H 5.05, N 5.40; found: C 89.12, H 4.74, N 5.18.

N,N′-*Bis-biphenyl-4-yl-9-ethyl*-N,N′-*di-pyren-1-yl-9*H-*carbazole-2,7-diamine* (**10**): Yellow solid. Yield: 67 %. FAB MS: *m/z* 929 (M^+). ^{1}H NMR (acetone-d_6, δ): 8.32–8.25 (m, 6H, pyrenyl), 8.22–8.14 (m, 6H, pyrenyl), 8.06–8.00 (m, 4H, pyrenyl), 7.95–7.92 (m, 4H, pyrenyl and C_6H_3), 7.61 (d, J = 7.3 Hz, 4H, *ortho*-C_6H_5), 7.54 (d, J = 8.7 Hz, 4H, C_6H_4) 7.37 (t, J = 7.8 Hz, 4H, *meta*-C_6H_5), 7.32 (d, J = 1.7 Hz, 2H, C_6H_3), 7.27 (t, J = 7.8 Hz, 2H, *para*-C_6H_5), 7.10 (d, J = 8.7 Hz, 4H, C_6H_4), 7.00 (dd, J = 8.3, 1.7 Hz, 2H, C_6H_3), 4.02 (q, J = 7.0 Hz, 2H, CH_2), 1.04 (t, J = 7.0 Hz, 3 H, CH_3). Anal. Calcd for $C_{70}H_{47}N_3$: C 90.39, H 5.09, N 4.52; found: C 89.90, H 4.84, N 4.10.

9-Ethyl-N,N′-*bis-(9-ethyl-9*H-*carbazol-3-yl)*-N,N′-*diphenyl-9*H-*carbazole-2,7-diamine* (**11**): Pale-yellow solid. Yield: 78 %. FAB MS: *m/z* 763 (M^+). ^{1}H NMR (acetone-d_6, δ): 7.99–7.97 (m, 4H, C_6H_4 and C_6H_3), 7.88 (d, J = 8.3 Hz, 2H, C_6H_3), 7.54–7.51 (m, 4H, C_6H_3), 7.42 (t, J = 8.2 Hz, 2H, C_6H_4), 7.31 (dd, J = 8.2, 1.7 Hz, 2H, C_6H_3), 7.22–7.18 (m, 6H, *meta*-C_6H_5 and C_6H_4), 7.11 (t, J = 8.2 Hz, 2H, C_6H_4), 7.06 (d, J = 8.2 Hz, 4H, *ortho*-C_6H_5), 6.94–6.88 (m, 4H, *para*-C_6H_5 and C_6H_3), 4.45 (q, J = 7.1 Hz, 4H, CH_2), 4.03 (q, J = 7.1 Hz, 2H, CH_2), 1.40 (t, J = 7.1 Hz, 6H, CH_3), 1.11 (t, J = 7.1 Hz, 3H, CH_3). Anal. Calcd for $C_{54}H_{45}N_5$: C 84.90, H 5.94, N 9.17; found: C 84.86, H 6.24, N 8.70.

9-Ethyl-N,N′-*bis[(2′,7′-di-*tert*-butyl)-9,9′-spirobifluoren-2-yl]*-N,N′-*diphenyl-9*H-*carbazole-2,7-diamine* (**12**): White solid. Yield: 80 %. FAB MS: *m/z* 1229 (M^+). ^{1}H NMR (acetone-d_6, δ): 7.89–7.86 (m, 4H, spirobifluorene), 7.75 (d, J = 8.3 Hz, 2H, C_6H_3), 7.70 (d, J = 7.8 Hz, 4H, spirobifluorene), 7.39–7.35 (m, 6H, spirobifluorene), 7.11–7.04 (m, 8H, spirobifluorene and *ortho*-C_6H_5), 7.01 (d, J = 1.7 Hz, 2H, C_6H_4), 6.91–6.87 (m, 6H, *ortho*- and *para*-C_6H_5), 6.79 (d, J = 1.6 Hz, 4H, *H*1′ and *H*8′ of spirobifluorene), 6.75 (dd, J = 8.3, 1.7 Hz, 2H, C_6H_4), 6.60 (d, J = 7.5 Hz, 2H, spirobifluorene), 6.49 (d, J = 2.0 Hz, 2H, spirobifluorene), 3.98 (q, J = 7.3 Hz, 2H, CH_2), 1.18 (s, 36H), 1.04 (t, J = 7.1 Hz, 3H, CH_3). Anal. Calcd for $C_{92}H_{83}N_3$: C 89.79, H 6.80, N 3.41; found: C 89.70, H 6.46, N 3.26.

9-Ethyl-N,N′-*bis-(6-cyano-9-ethyl-9*H-*carbazol-3-yl)*-N,N′-*di(naphthalen-1-yl)-9*H-*carbazole-2,7-diamine* (**13**): Yellow-green solid. Yield: 82 %. FAB MS: *m/z* 913 (M^+). ^{1}H NMR (acetone-d_6, δ): 8.46 (d, J = 0.9 Hz, 2H, C_6H_3), 8.12–8.08 (m, 4H, $C_{10}H_7$), 7.96 (d, J = 8.1 Hz, 2H, C_6H_3)7.81 (t, J = 7.5 Hz, 4H, $C_{10}H_7$), 7.71 (d, J = 1.0 Hz, 4H, C_6H_3), 7.60 (d, J = 8.4 Hz, 2H, C_6H_3), 7.52 (t, J = 7.5 Hz, 2H, $C_{10}H_7$), 7.46 (t, J = 7.0 Hz, 2H, $C_{10}H_7$), 7.40–7.31 (m, 6H, $C_{10}H_7$ and C_6H_3), 7.00 (d, J = 1.7 Hz, 2H, C_6H_3), 6.77 (dd, J = 8.4, 1.8 Hz, 2H, C_6H_3), 4.53 (q, J = 7.2 Hz, 4H, CH_2), 3.86 (q, J = 7.1 Hz, 2H, CH_2), 1.43 (t, J = 7.0 Hz, 6H, CH_3), 0.95 (t, J = 6.9 Hz, 3H, CH_3). Anal. Calcd for $C_{64}H_{47}N_7$: C 84.09, H 5.18, N 10.73; found: C 83.61, H 4.97, N 10.47.

4.2.5. 2,7-Bis[5-(N,N-diphenylamino)-2-thienyl]-9-ethyl-9H-carbazole (**16**)

To a mixture of diphenyl-(5-tributylstannanyl-thiophen-2-yl)-amine (0.78 g, 1.3 mmol, 90 % purity), compound **5** (0.18 g, 0.5 mmol) and $PdCl_2(PPh_3)_2$ (14 mg, 0.02 mmol) was added 4 mL of dry dimethylformamide (DMF). The solution was slowly warmed to 80 °C and stirred for 24 h. After cooling, methanol (5 mL) was added to precipitate the product. The solid was filtered, washed with methanol (2 × 5 mL), and then chromatographed using dichloromethane/hexanes as eluent. Compound **16** was obtained as yellow solid in 83 % yield. FAB MS: *m/z* 693 (M^+). ^{1}H NMR (acetone-d_6, δ): 8.10 (d, J = 8.0 Hz, 2H, C_6H_3), 7.76 (s, 2H, C_6H_3), 7.47 (dd, J = 8.0, 1.3 Hz, 2H, C_6H_3), 7.43 (d, J = 3.8 Hz, 2H, SC_4H_2), 7.34 (t, J = 7.4 Hz, 8H, *meta*-C_6H_5), 7.18 (d, J = 7.4 Hz, 8H, *ortho*-C_6H_5), 7.09 (t, J = 7.4 Hz, 4H, *para*-C_6H_5), 6.75

(d, $J = 3.8$ Hz, 2H, SC_4H_2), 4.57 (q, $J = 7.1$ Hz, 2H, CH_2), 1.43 (t, $J = 7.1$ Hz, 3H, CH_3). Anal. Calcd for $C_{46}H_{35}N_3S_2$: C 79.62, H 5.08, N 6.06; found: C 79.21, H 5.18, N 5.97.

4.3. LED Fabrication and Measurements

Electron-transporting materials TPBI (1,3,5-tris(*N*-phenylbezimidazol-2-yl)benzene) and Alq_3 (tris(8-hydroxyquinoline) aluminum) were synthesized according to literature procedures [33], and were sublimed twice prior to use. Prepatterned ITO substrates with an effective individual device area of 3.14 mm^2 were cleaned as described in a previous report [34]. Double-layer EL devices using compounds **2**–**3**, **7**, **9**–**11**, **13**, and **15**–**16** as the hole-transport and emitting layer and TPBI or Alq_3 as the electron-transport layer were fabricated. The devices were prepared by vacuum deposition of 40 nm of the hole-transporting layer, followed by 40 nm of TPBI or Alq_3. An alloy of magnesium and silver (ca. 10:1, 50 nm) was deposited as the cathode, which was capped with 100 nm of silver. *I*–*V* curves were measured on a Keithley 2400 Source Meter in ambient environment. Light intensity was measured with a Newport 1835 Optical Meter.

4.4 Time-of-Flight (TOF) Mobility Measurement

The compounds **7**, **9**, and their 3,6-substituted analogues **7A**, **9A** (Fig. 1) [7a] were subjected to TOF mobility studies. They were purified by sublimation before use in subsequent analyses and device fabrication. The samples *x* (*x* = **7**, **9**, **7A**, or **9A**) for the TOF measurement were prepared by vacuum deposition using the following structure: glass/Ag (30 nm)/*x* (ca. 2 μm)/Al (150 nm) with an active area of 2×2 mm as described in a previous report [35]. A frequency-tripled Nd:YAG (YAG: yttrium aluminum garnet) laser (355 nm) with a pulse duration of ca. 10 ns was used for pulsed illumination through the semitransparent Ag. Under an applied dc bias, the transient photocurrent as a function of time was recorded with a digital storage oscilloscope. The TOF measurements were typically performed in a 10^{-5} Torr vacuum chamber. Depending on the polarity of the applied bias *V*, selected photogenerated carriers (holes or electrons) were swept across the sample thickness *D* with a transit time t_T, the applied electric field *E* was then *V*/*D*, and the carrier mobility was given by $\mu = D/(t_T \cdot E) = D^2/(V \cdot t_T)$.

Received: October 5, 2006
Revised: November 6, 2006
Published online: February 5, 2007

[1] a) Y. Shirota, *J. Mater. Chem.* **2000**, *10*, 1. b) P. Lu, H. Hong, G. Cai, P. Djurovich, W. P. Weber, M. E. Thompson, *J. Am. Chem. Soc.* **2000**, *122*, 7480. c) Y. Shirota, M. Kinoshita, T. Noda, K. Okumoto, T. Ohara, *J. Am. Chem. Soc.* **2000**, *122*, 11 021. d) A. W. Freeman, S. C. Koene, P. R. L. Malenfant, M. E. Thompson, J. M. J. Fréchet, *J. Am. Chem. Soc.* **2000**, *122*, 12 385. e) C. Wang, G.-Y. Jung, Y. Hua, C. Pearson, M. R. Bryce, M. C. Petty, A. S. Batsanov, A. E. Goeta, J. A. K. Howard, *Chem. Mater.* **2001**, *13*, 1167. f) Y.-T. Tao, E. Balasubramian, A. Danel, B. Jarosz, P. Tomasik, *Chem. Mater.* **2001**, *13*, 1207.

[2] a) W. J. Ni, J. H. Su, K. Chen, H. Tian, *Chem. Lett.* **1997**, 101. b) W. H. Zhu, C. Hu, K. C. Chen, H. Tian, *Synth. Met.* **1998**, *96*, 151. c) U. Mitschke, P. Bäuerle, *J. Mater. Chem.* **2000**, *10*, 1471. d) J. Pei, W.-L. Yu, W. Huang, A. J. Heeger, *Macromolecules* **2000**, *33*, 2462. e) S. Liu, X. Jiang, H. Ma, M. S. Liu, A. K.-Y. Jen, *Macromolecules* **2000**, *33*, 3514. f) T. Miteva, A. Meisel, W. Knoll, H. G. Nothofer, U. Scherf, D. C. Müller, K. Meerholz, A. Yasuda, D. Neher, *Adv. Mater.* **2001**, *13*, 565. g) C. Wang, M. Kilitziraki, L.-O. Pålsson, M. R. Bryce, A. P. Monkman, I. D. W. Samuel, *Adv. Funct. Mater.* **2001**, *11*, 47.

[3] C. W. Tang, S. A. Van Slyke, *Appl. Phys. Lett.* **1987**, *51*, 913.

[4] J. H. Burroughes, D. D. C. Bradley, A. R. Brown, R. N. Marks, K. MacKay, R. H. Friend, P. L. Burn, A. B. Holmes, *Nature* **1990**, *347*, 539.

[5] P. Fenter, F. Schreiber, V. Bulovic, S. R. Forrest, *Chem. Phys. Lett.* **1997**, *277*, 521.

[6] B. E. Koene, D. E. Loy, M. E. Thompson, *Chem. Mater.* **1998**, *10*, 2235.

[7] a) K. R. Justin Thomas, J. T. Lin, Y.-T. Tao, C.-W. Ko, *Adv. Mater.* **2000**, *12*, 1949. b) K. R. Justin Thomas, J. T. Lin, Y.-T. Tao, C.-W. Ko, *J. Am. Chem. Soc.* **2001**, *123*, 9404. c) K. R. Justin Thomas, J. T. Lin, Y.-T. Tao, C.-H. Chuen, *Chem. Mater.* **2002**, *14*, 3852.

[8] a) O. Paliulis, J. Ostrauskaite, V. Gaidelis, V. Jankauskas, P. Strohriegl, *Macromol. Chem. Phys.* **2003**, *204*, 1706. b) M. Sonntag, P. Strohriegl, *Chem. Mater.* **2004**, *16*, 4736.

[9] a) Y.-H. Niu, J. Huang, Y. Cao, *Adv. Mater.* **2003**, *15*, 807. b) Y. Li, J. Ding, M. Day, Y. Tao, J. Lu, M. D'iorio, *Chem. Mater.* **2004**, *16*, 2165. c) S. Grigalevicius, *Synth. Met.* **2006**, *156*, 1.

[10] a) J.-F. Morin, M. Leclerc, *Macromolecules* **2001**, *34*, 4680. b) J.-F. Morin, P.-L. Boudreault, M. Leclerc, *Macromol. Rapid Commun.* **2002**, *23*, 1032. c) G. Zotti, G. Schiavon, S. Zecchin, J.-F. Morin, M. Leclerc, *Macromolecules* **2002**, *35*, 2122. d) J.-F. Morin, M. Leclerc, *Macromolecules* **2002**, *35*, 8413. e) J.-F. Morin, M. Leclerc, D. Adès, A. Siove, *Macromol. Rapid Commun.* **2005**, *26*, 761.

[11] F. Dierschke, A. C. Grimsdale, K. Müllen, *Synthesis* **2003**, 2470.

[12] a) J. F. Hartwig, *Synlett* **1997**, 329. b) M. Nishiyama, T. Yamamoto, Y. Koie, *Tetrahedron Lett.* **1998**, *39*, 617. c) J. F. Hartwig, *Angew. Chem. Int. Ed.* **1998**, *37*, 2047.

[13] P. Kundu, K. R. Justin Thomas, J. T. Lin, Y.-T. Tao, C.-H. Chuen, *Adv. Funct. Mater.* **2003**, *13*, 445.

[14] D. F. O'Brien, P. E. Burrows, S. R. Forrest, B. E. Koene, D. E. Loy, M. E. Thompson, *Adv. Mater.* **1998**, *10*, 1108.

[15] J. Y. Shen, C. Y. Lee, T.-H. Huang, J. T. Lin, Y.-T. Tao, C.-H. Chien, *J. Mater. Chem.* **2005**, *15*, 2455.

[16] a) J. Salbeck, N. Yu, J. Bauer, F. Weissörtel, H. Bestgen, *Synth. Met.* **1997**, *91*, 209. b) K. H. Weinfurtner, F. Weissörtel, G. Harmgarth, J. Salbeck, *Proc. SPIE-Int. Soc. Opt. Eng.* **1998**, *3476*, 40.

[17] a) K. Naito, A. Miura, *J. Phys. Chem.* **1993**, *97*, 6240. b) K. Naito, *Chem. Mater.* **1994**, *6*, 2343.

[18] S. Wang, W. J. Oldham, Jr., R. A. Hudack, Jr., G. C. J. Bazan, *J. Am. Chem. Soc.* **2000**, *122*, 5695.

[19] The thermal decomposition temperature of **7A** was incorrect in our previous report (ref. [7b]). It was remeasured and the correct value is reported here.

[20] a) W. D. Gill, *J. Appl. Phys.* **1972**, *43*, 5033. b) H. Bässler, *Philos. Mag. B* **1992**, *65*, 795. c) H. Bässler, *Int. J. Mod. Phys. B* **1994**, *8*, 847.

[21] Y. Li, M. K. Fung, Z. Xie, S. T. Lee, L.-S. Hung, J. Shi, *Adv. Mater.* **2002**, *14*, 1317.

[22] a) K. R. Justin Thomas, M. Velusamy, J. T. Lin, Y.-T. Tao, C.-H. Chuen, *Adv. Funct. Mater.* **2004**, *14*, 387. b) S. Grigalevicius, *Synth. Met.* **2006**, *156*, 1.

[23] C. Adachi, R. kwong, S. R. Forrest, *Org. Electron.* **2001**, *2*, 37.

[24] A. P. Kulkarni, C. J. Tonzola, A. Babel, S. A. Jenehke, *Chem. Mater.* **2004**, *16*, 4556.

[25] J. Pommerehne, H. Vestweber, W. Guss, R. F. Mahrt, H. Bässler, M. Porsch, J. Daub, *Adv. Mater.* **1995**, *7*, 551.

[26] a) X. H. Zhang, W. Y. Lai, Z. Q. Gao, T. C. Wong, C. S. Lee, H. L. Kwong, S. T. Lee, S. K. Wu, *Chem. Phys. Lett.* **2000**, *320*, 77. b) Y. T. Tao, E. Balasubramaniam, A. Danel, P. Tomasik, *Appl. Phys. Lett.* **2000**, *77*, 933.

[27] R. C. Kwong, S. Lamansky, M. E. Thompson, *Adv. Mater.* **2000**, *12*, 1134.

[28] F.-I. Wu, P.-I. Shih, M.-C. Yuan, A. K. Dixit, C.-F. Shu, Z.-M. Chung, E. W.-G. Diau, *J. Mater. Chem.* **2005**, *15*, 4753.

[29] R. D. Hreha, C. P. George, A. Haldi, B. Domercq, M. Malagoli, S. Barlow, J.-L. Brédas, B. Kippelen, S. R. Marder, *Adv. Funct. Mater.* **2003**, *13*, 967.

[30] G. Jones II, W. R. Jackson, C.-Y. Choi, W. R. Bergmark, *J. Phys. Chem.* **1985**, *89*, 294.

[31] Y.-Z. Su, J. T. Lin, Y.-T. Tao, C.-W. Ko, S.-C. Lin, S.-S. Sun, *Chem. Mater.* **2002**, *14*, 1884.

ADVANCED FUNCTIONAL MATERIALS

[32] P.-H. Huang, J.-Y. Shen, S.-C. Pu, Y.-S. Wen, J. T. Lin, P.-T. Chou, M.-C. P. Yeh, *J. Mater. Chem.* **2006**, *16*, 850.

[33] a) A. Y. Sonsale, S. Gopinathan, C. Gopinathan, *Indian J. Chem.* **1976**, *14*, 408. b) J. Shi, C. W. Tang, C. H. Chen, *US Patent 5 645 948*, **1997**. c) C. H. Chen, J. Shi, *Coord. Chem. Rev.* **1998**, *171*, 161.

[34] E. Balasubramaniam, Y. T. Tao, A. Danel, P. Tomasik, *Chem. Mater.* **2000**, *12*, 2788.

[35] a) P. M. Borsenberger, D. S. Weiss, *Organic Photoreceptors for Imaging Systems*; Marcel Dekker, New York **1993**. b) C.-C. Wu, T.-L. Liu, W.-Y. Hung, Y.-T. Lin, K.-T. Wong, R.-T. Chen, Y.-M. Chen, Y.-Y. Chien, *J. Am. Chem. Soc.* **2003**, *125*, 3710. c) C.-C. Wu, W.-Y. Hung, T.-L. Liu, L.-Z. Zhang, T.-Y. Luh, *J. Appl. Phys.* **2003**, *93*, 5465. d) C.-C. Wu, T.-L. Liu, Y.-T. Lin, W.-Y. Hung, T.-H. Ke, K.-T. Wong, T.-C. Chao, *Appl. Phys. Lett.* **2004**, *85*, 1172. e) C.-C. Wu, W.-G. Liu, W.-Y. Hung, T.-L. Liu, Y.-T. Lin, H.-W. Lin, K.-T. Wong, Y.-Y. Chien, R.-T. Chen, T.-H. Hung, T.-C. Chao, Y.-M. Chen, *Appl. Phys. Lett.* **2005**, *87*, 052 103. f) L.-Y. Chen, W.-Y. Hung, Y.-T. Lin, C.-C. Wu, T.-C. Chao, T.-H. Hung, K.-T. Wong, *Appl. Phys. Lett.* **2005**, *87*, 112 103. g) W.-Y. Hung, T.-H. Ke, Y.-T. Lin, C.-C. Wu, T.-H. Hung, T.-C. Chao, K.-T. Wong, C.-I. Wu, *Appl. Phys. Lett.* **2006**, *88*, 64 102.